

 Open access • Posted Content • DOI:10.1101/2021.04.27.441663

## **Sustained coevolution of phage Lambda and Escherichia coli involves inner as well as outer membrane defenses and counter-defenses** — [Source link](#)

Alita R. Burmeister, Rachel M. Sullivan, Jenna Gallie, Richard E. Lenski

**Institutions:** Yale University, University of Wisconsin-Madison, Max Planck Society, Michigan State University

**Published on:** 28 Apr 2021 - bioRxiv (Cold Spring Harbor Laboratory)

**Topics:** Bacterial outer membrane and Lambda phage

Related papers:

- [Sustained coevolution of phage Lambda and Escherichia coli involves inner- as well as outer-membrane defences and counter-defences.](#)
- [Bacteriophage adaptation to a mammalian mucosa reveals a trans-domain evolutionary axis](#)
- [Multiple mechanisms drive phage infection efficiency in nearly identical hosts.](#)
- [Impact of Xenogeneic Silencing on Phage-Host Interactions.](#)
- [Bacteriophage-host interactions in assembly.](#)

Share this paper:    

View more about this paper here: <https://typeset.io/papers/sustained-coevolution-of-phage-lambda-and-escherichia-coli-26vcfp1k9s>

1 **Sustained coevolution of phage Lambda and *Escherichia coli***  
2 **involves inner as well as outer membrane defenses and counter-**  
3 **defenses**

4 Alita R. Burmeister,<sup>1,2,#,\*</sup> Rachel M. Sullivan,<sup>1,2\*\*</sup> Jenna Gallie,<sup>3,4,5\*\*\*</sup> and Richard  
5 E. Lenski<sup>1,2</sup>

6

7 <sup>1</sup>Department of Microbiology and Molecular Genetics, Michigan State University, East  
8 Lansing, MI, USA

9 <sup>2</sup>BEACON Center for the Study of Evolution in Action, Michigan State University, East  
10 Lansing, MI, USA

11 <sup>3</sup>Department of Biology, University of Washington, Seattle, WA, USA

12 <sup>4</sup>Department of Environmental Microbiology, Eawag, Dübendorf, Switzerland

13 <sup>5</sup>Department of Environmental Systems Science, ETH Zürich, Zürich, Switzerland

14

15 **Running Head:** Bacteria-phage coevolution

16 **#Correspondence:** Alita R. Burmeister, [alita.burmeister@yale.edu](mailto:alita.burmeister@yale.edu)

17 **\*Present address:** Department of Ecology and Evolutionary Biology, Yale University,  
18 New Haven, CT, USA

19 **\*\*Present address:** Waisman Center, University of Wisconsin, Madison, WI, USA

20 **\*\*\*Present address:** Department of Evolutionary Theory, Max Planck Institute for  
21 Evolutionary Biology, 24306 Plön, Germany

22

23 **Word count for the abstract:** 185 words

24 **Word count for the text:** 2,682 words

25 **Abstract**

26 Bacteria often evolve resistance to phage through the loss or modification of cell-surface  
27 receptors. In *Escherichia coli* and phage  $\lambda$ , such resistance can catalyze a coevolutionary  
28 arms race focused on host and phage structures that interact at the outer membrane. Here,  
29 we analyze another facet of this arms race involving interactions at the inner membrane,  
30 whereby *E. coli* evolves mutations in mannose permease-encoding genes *manY* and *manZ*  
31 that impair  $\lambda$ 's ability to eject its DNA into the cytoplasm. We show that these *man*  
32 mutants arose concurrently with the arms race at the outer membrane. We tested the  
33 hypothesis that  $\lambda$  evolved an additional counter-defense that allowed them to infect  
34 bacteria with deleted *man* genes. The deletions severely impaired the ancestral  $\lambda$ , but  
35 some evolved phage grew well on the deletion mutants, indicating they regained  
36 infectivity by evolving the ability to infect hosts independently of the mannose permease.  
37 This coevolutionary arms race fulfills the model of an inverse-gene-for-gene infection  
38 network. Taken together, the interactions at both the outer and inner membranes reveal  
39 that coevolutionary arms races can be richer and more complex than is often appreciated.

40

41 **IMPACT STATEMENT**

42 Laboratory studies of coevolution help us understand how host defenses and pathogen  
43 counter-defenses change over time, which is often essential for predicting the future  
44 dynamics of host-pathogen interactions. One particular model, termed “inverse-gene-for-  
45 gene” coevolution, predicts that coevolution proceeds through alternating steps, whereby  
46 hosts lose the features exploited by pathogens, and pathogens evolve to exploit  
47 alternative features. Using a classic model system in molecular biology, we describe the

48 nature and timing of a previously overlooked step in the coevolution of *E. coli* and  
49 bacteriophage lambda. Our work demonstrates that this mode of coevolution can  
50 profoundly re-shape the interactions between bacteria and phage.

51

## 52 **INTRODUCTION**

53 An issue of longstanding interest is whether the coevolution of bacteria and virulent  
54 (lytic) phages involves endless rounds of bacterial defenses and phage counter-defenses.  
55 Based on experiments in chemostats, Lenski and Levin (1) suggested that bacteria  
56 typically had the upper hand, as *Escherichia coli* often eventually evolved resistance by  
57 deleting or inactivating the phage's specific receptor, which the phage could not readily  
58 overcome. This resistance did not imply the extinction of the phage, however, because it  
59 often reduced the bacteria's competitiveness for resources. Instead, the typical outcome  
60 was coexistence of resistant and sensitive bacteria, with the latter more efficient at  
61 exploiting resources and thus able to sustain the phage's persistence (2, 3). A study of  
62 cyanobacteria and their phages in the marine environment also supported this pattern (4).

63 On the other hand, Lenski and Levin also pointed out that bacteria would lose the  
64 upper hand if the phage targeted a receptor that was essential for the bacteria to survive in  
65 their current environment. They cited then-recent work by Williams Smith & Huggins (5,  
66 6), who showed they could successfully treat mice with otherwise lethal bacterial  
67 infections using a phage that specifically targeted a receptor required for the bacteria to  
68 colonize the mice. As the problem of bacterial resistance to antibiotics has grown, similar  
69 strategies are now being tested in which phage that specifically target drug-efflux pumps  
70 are deployed as therapeutic agents (7-9). In the meantime, yet other forms of bacteria-

71 phage coevolution have been discovered, including CRISPR systems in bacteria and  
72 countermeasures to avoid these defenses in phage (10-13).

73 Another part of the argument that bacteria had the upper hand in the coevolutionary  
74 arms race depended on the idea that, while phages could often counter minor mutations in  
75 receptors, it was much more difficult for them to evolve the ability to use another  
76 receptor if the bacteria simply stopped producing the usual receptor (1). However, more  
77 recent work has shown that some host-phage pairs can undergo longer coevolutionary  
78 cycles involving defenses and counter-defenses at the outer membrane (14-16), and some  
79 phages can evolve to use new receptors even on a short time scale (17). This  
80 coevolutionary dynamic – in which hosts lose structures exploited by specific pathogens,  
81 and those pathogens evolve to exploit alternative structures – is called inverse-gene-for-  
82 gene (IGFG) coevolution (18-21). This IGFG framework is useful for representing  
83 changes in coevolving communities of bacteria and phage (Fig. 1). For example, if phage  
84 cannot evolve to exploit new features after bacteria have evolved resistance, then phage  
85 populations may be evolutionarily static (22, 23). Conversely, if phage exploit essential  
86 features of the bacteria that cannot be eliminated, then the host's evolution is constrained  
87 and phage infectivity may remain elevated (6, 8). Our study builds on one such example  
88 of IGFG coevolution, in which it was discovered that populations of a virulent strain of  
89 phage  $\lambda$  often evolved the ability to use another outer-membrane receptor after  
90 coevolving *E. coli* reduced their expression of the receptor that the phage had initially  
91 exploited (17, 24).

92 Phage  $\lambda$  requires a two-step infection process to cross the outer and inner bacterial  
93 membranes (Fig. S1). The  $\lambda$  tail initiates infection at the outer membrane of the cell,

94 where its J protein fibers adsorb to the bacterial protein LamB (25, 26). The tail proteins  
95 V and H allow  $\lambda$  to enter the periplasm and thereby interact with the mannose permease  
96 proteins (encoded by *manY* and *manZ*) in the inner membrane, which  $\lambda$  uses to eject its  
97 genome into the cytoplasm (27-30). Resistance to  $\lambda$  can occur by blocking  $\lambda$ 's entry at  
98 either the outer or inner membrane, with resistance mutations typically mapping to *lamB*,  
99 *lamB*'s positive regulator *maltT* (25, 26), or the mannose permease genes (27, 28, 30)  
100 (Fig. S1). It has been shown that sensitive *E. coli* and lytic  $\lambda$  can coexist, along with  
101 resistant *E. coli* mutants, in both continuous (31) and batch culture regimes (17). Previous  
102 analysis of this coevolving system has revealed IGFG dynamics focused on outer  
103 membrane defenses and counter-defenses. That is, *E. coli* often first evolves *maltT*  
104 mutations that reduce LamB expression, resulting in increased resistance to  $\lambda$  (17, 31,  
105 32), and  $\lambda$  then regains infectivity through mutations in the *J* gene that increase its  
106 adsorption rate and fitness (31, 33). In some, but not all, experiments, specific sets of *J*  
107 mutations allow the novel exploitation of a second outer membrane protein, OmpF,  
108 catalyzing further evolution including mutations in the *ompF* gene (17, 34).

109 Despite extensive knowledge about the evolution of the initial (adsorption) and final  
110 (lysis) steps of  $\lambda$  infection of *E. coli*, much less is known about the evolution of the  
111 genetic networks during other stages of infection, including  $\lambda$ 's passage through the  
112 periplasmic space and the ejection of its DNA into the host cytoplasm. Meyer *et al.* (17)  
113 found that *E. coli* coevolving with  $\lambda$  often acquired mutations that impacted their ability  
114 to grow on mannose, which presumably were favored because they disrupt entry of the  
115 phage genome via the mannose permease. In this study, we examine how this  
116 coevolutionary arms race – previously focused on the cell's outer membrane – also set off

117 an arms race involving the host's inner membrane, including the mechanism  $\lambda$  uses to  
118 eject its DNA through that membrane and into the bacteria's cytoplasm.

119

## 120 **METHODS**

### 121 **Bacteria and phage strains**

122 Meyer *et al.* (17) founded 96 replicate cultures with *E. coli* B strain REL606 and lytic  
123 phage  $\lambda$  cI26, serially passaged the communities for 20 days, and froze mixed-  
124 community samples daily. Some of the phage populations evolved the ability to use the  
125 outer membrane protein OmpF as a receptor, some of the bacterial populations evolved  
126 mutations that affected mannose metabolism, and some communities changed in both  
127 respects. We obtained phage isolates from two of the populations (Table 1, Pop-A and  
128 Pop-B) that changed in both of these key respects; in each case, however, the isolates  
129 were taken four days before the phage had evolved the new ability to use the OmpF  
130 receptor (Table 1, Supplementary Material). *E. coli* K12 strains BW25113, JW1807, and  
131 JW1808 are from the Keio collection (35). REL606  $\Delta manZ$  was constructed using a two-  
132 step allelic exchange (Supplementary Material, Table S1, and Table S2).

### 133 **Phage growth assays**

134 We measured the population growth of the ancestral and evolved phages under the same  
135 culture conditions as those in which the communities evolved (17) (Supplementary  
136 Material). The initial densities were  $\sim 9 \times 10^6$  cells per ml and  $\sim 1 \times 10^4$  phage per ml. We  
137 calculate the phage's net population growth as the ratio of its final density after one day  
138 to its initial density; we show the resulting net growth on a  $\log_{10}$ -transformed scale. We  
139 enumerated the initial and final phage populations using dilution plating and soft-agar

140 overlays (Supplementary Material). We performed 5 or 6 replicate assays for each phage-  
141 host combination shown in Figure 2.

### 142 **Frequency of mutants with altered mannose phenotypes**

143 We estimated the frequency of bacteria with mutations affecting the mannose permease  
144 by plating from the time-series of frozen samples taken from populations Pop-A and Pop-  
145 B on tetrazolium mannose agar, as done previously (17). Mutants with reduced ability to  
146 metabolize mannose form deeply pigmented colonies that can be readily distinguished  
147 from those of the ancestral strain REL606, which forms light pink colonies on that  
148 medium.

149 *Data accessibility:* Data are available as Supplementary Datasets S1 (net population  
150 growth of phage  $\lambda$  on wild type and knockout bacteria) and S2 (temporal dynamics of  
151 *man* mutants in *E. coli* populations).

152

## 153 **RESULTS AND DISCUSSION**

154 Our experiments focus on two independently coevolved communities of mixed *E. coli*  
155 and  $\lambda$  populations, designated Pop-A and Pop-B (17). Both  $\lambda$  populations evolved from a  
156 common ancestral phage (strain cI26). From each evolved population, we isolated a  
157 single phage clone:  $\lambda$ -A from Pop-A and  $\lambda$ -B from Pop-B (Table 1). Each clone was  
158 isolated 4 days before its population evolved the ability to use the OmpF receptor; hence,  
159 the phage clones were isolated on different days of the coevolution experiment performed  
160 by Meyer et al. (17).

161 To examine whether and how coevolution affected  $\lambda$ 's dependence on the ManY and  
162 ManZ proteins, we measured the population growth of the ancestral (cI26) and the two



163 coevolved phage isolates ( $\lambda$ -A and  $\lambda$ -B) on bacterial strains with and without the *manY*  
164 and *manZ* genes (Table 1). Both the ancestral and evolved phage isolates grew well on  
165 bacterial strains with intact *manY* and *manZ* genes, including both the ancestral *E. coli* B  
166 strain, REL606, used in the coevolution experiment, and the K12 genetic background in  
167 which the Keio collection was made (Fig. 2, Table 1). Deletion of either the *manY* or  
168 *manZ* gene in either background severely reduced the ancestral phage's population  
169 growth. In two cases (REL606  $\Delta$ *manZ* and Keio  $\Delta$ *manY*), we saw no growth whatsoever  
170 in the ancestral phage (cI26) population after 24 hours; in the other case (Keio  $\Delta$ *manZ*),  
171 the ancestral phage population increased ~10-fold, but that was five orders of magnitude  
172 less than the increase on the same background with both mannose permease genes  
173 present. In striking contrast, both evolved phage isolates showed substantial growth on all  
174 three bacterial strains that lacked either the *manY* or *manZ* gene (Fig. 2). These results  
175 thus indicate an inverse-gene-for-gene coevolutionary interaction at the inner membrane.  
176 That is, the bacteria modified or lost the mannose permease, which the ancestral phage  
177 used to eject its genome into the cytoplasm, and the phage countered by evolving  
178 independence of that function.

179 To determine when the mutant mannose permease mutants arose in the two *E. coli*  
180 populations studied here, we plated frozen samples from the coevolution experiments on  
181 tetrazolium mannose agar, on which *man* mutants form pigmented colonies  
182 distinguishable from the wild type (Supplementary Material) (36). We are particularly  
183 interested in the timing of the appearance of the *man* mutants relative to two other steps  
184 in the coevolutionary arms race that were previously characterized: (i) the *maltT*  
185 mutations that reduced the bacteria's expression of LamB and thus the adsorption of the

186 ancestral phage (33); and (ii)  $\lambda$ 's new ability to adsorb to OmpF as an alternative receptor  
187 (17). Our phage-growth data demonstrate that *manY* and *manZ* deletions confer  
188 substantial resistance even to the ancestral phage, which can use only the LamB surface  
189 receptor (Fig. 2). That result suggests the possibility that the *man* mutants could have  
190 arisen early in the coevolution experiments, perhaps alongside or even before the *maltT*  
191 mutations that provided resistance at the outer membrane. However, time-course data  
192 show that the *man* alleles consistently reached high frequencies (above the detection  
193 limits, shown as gray dashed lines in Fig. 3) only after the fixation of the *maltT* mutations,  
194 which occurred by day 8 in both populations studied here (17) (Fig. 3, Fig. 4, Table S3).

195 These temporal data also show that the *man* mutations had nearly fixed in both  
196 bacterial populations (frequencies >95% on day 10 in Pop-A and on day 12 in Pop-B),  
197 but then the mutants sharply declined the next day. This reversal suggests these mutants  
198 were killed by phages that evolved independence of the mannose permease, and it is  
199 consistent with previous data showing that mutant *man* alleles rarely fixed in the bacterial  
200 populations (17). Meyer et al. (Fig. S2 in (17)) reported that the bacterial population  
201 densities remained high ( $\sim 2 \times 10^9$  cells per ml, near the carrying capacity of the medium)  
202 throughout this period of the evolution experiment. Therefore, the mutant frequencies  
203 that we observed (Fig. 3) correspond to  $\sim 4 \times 10^7$  cells per ml (about 2% of the total  
204 population, the limit of detection in that assay) to almost  $2 \times 10^9$  cells per ml (the  
205 carrying capacity). With such large population sizes, any phage mutants that gained the  
206 ability to infect the *man* mutants would have access to a large number of hosts, and  
207 correspondingly, a large fitness benefit. The resulting growth of the *man*-independent  
208 phage population would drive the frequency of *man* mutants down, especially if the *man*-

209 independent phages preferentially infected and killed the *man* mutants relative to other  
210 cells that retained the wild-type permease. Fitness costs associated with loss of the  
211 mannose permease may also have contributed to the reversal, although the costs of the  
212 resistance mutations are small compared to their benefit in the presence of phage (36).

213 In host Pop-A, variation in colony morphology further suggested that different *man*  
214 alleles were present before and after the sudden decline in the frequency of *man* mutants  
215 on day 11 (Fig. 4, Supplementary Material). The initial boom and bust of the mutant *man*  
216 alleles in both populations also occurred before the phage had evolved to use OmpF (Fig.  
217 3, dashed arrows). Whether  $\lambda$  gained independence from the mannose permease by  
218 exploiting another inner membrane protein, and whether *E. coli* did (or could) respond by  
219 eliminating such a structure, are interesting questions for future work.

220 Our results are broadly consistent with genetic and molecular biology studies of  $\lambda$   
221 host-range mutations. Scandella and Arber (30) isolated *E. coli* mutants that allowed  
222 phage adsorption to the cell envelope but interfered with ejection of the phage genome,  
223 thereby reducing infection success to a small fraction of that observed on wild-type cells.  
224 The responsible mutations were mapped to the mannose permease operon (27, 37), and  $\lambda$   
225 mutants that could infect these mutant bacteria had mutations in phage genes *V* or *H* (38).  
226 Mutations in *V* and *H* have also been observed in another population in this study system  
227 (39). Williams *et al.* (37) found that, for *E. coli* strain K12, *manZ* is not strictly required  
228 for wild-type  $\lambda$  to eject its genome, and our results accord with that finding (Fig. 2, Keio  
229 background). However, our results suggest that  $\lambda$  cI26 does require *manZ* when infecting  
230 *E. coli* strain B, at least in the culture conditions that we used (Fig. 2, REL606  
231 background). Alternatively,  $\lambda$  cI26 might occasionally infect and replicate in hosts

232 without *manZ*, but at a rate that is offset by the decay or inactivation of free virus  
233 particles under these conditions (17, 33). In any case, the net population growth of the  
234 ancestral phage on either the  $\Delta manY$  or  $\Delta manZ$  bacteria is insufficient to offset the 100-  
235 fold daily dilutions (Fig. 2, dashed line) that took place during the coevolution  
236 experiment (17).

237 Taken together, our results imply that *E. coli* and  $\lambda$  coevolved in an inverse gene-for-  
238 gene manner (18) (Fig. 1). This coevolution involved two infection steps – crossing first  
239 the outer and then the inner membrane – and at least three, and probably four, distinct  
240 host features (Figs. 1, 5, and S1). *E. coli* evolved resistance to phage  $\lambda$  through the loss or  
241 alteration of maltose transport across the outer membrane (via mutations in *maltT*) and  
242 mannose transport across the inner membrane (via mutations in *manY* or *manZ*), while  $\lambda$   
243 evolved to exploit other *E. coli* features including another outer membrane protein  
244 (OmpF) and, presumably, some as yet unidentified, alternative inner membrane protein  
245 (shown as encoded by the hypothetical *imx* gene in Fig. 5). While our study addresses  
246 one particular bacteria-phage interaction in a simple laboratory setting, it illustrates the  
247 extent to which the resulting coevolutionary arms races can be richer and more complex  
248 than is often appreciated.

249 There are many alternative coevolutionary paths through an inverse-gene-for-gene  
250 network that has four features subject to host defenses and parasite counter-defenses (Fig.  
251 5). This multiplicity of potential paths suggests that mutation and selection could drive  
252 replicate communities to different regions of the coevolutionary landscape, raising other  
253 interesting questions. How might different first-step resistance mutations affect the  
254 subsequent host-range evolution of the phage and the further evolution of host resistance?

255 To what extent can IGFG systems continuously evolve host defenses and parasite  
256 counter-defenses? What is the effect of such prolonged coevolution for community  
257 diversity? Do communities become increasingly divergent as the coevolving populations  
258 follow different paths through the network, or might they eventually converge on the  
259 same phenotypic states after a period of divergence? How important are evolutionary  
260 innovations in opening new paths, relative to pleiotropic tradeoffs that may close off  
261 certain paths? Future work should investigate these and other questions about the  
262 coevolution of bacteria and phage and the structure of their genetic interaction networks.

263

#### 264 **FUNDING INFORMATION**

265 This work was supported by the National Science Foundation Graduate Research  
266 Fellowship (DGE-1424871) to A.R.B., the BEACON Center for the Study of Evolution  
267 in Action (NSF Cooperative Agreement DBI-0939454), the John Hannah endowment  
268 from Michigan State University to R.E.L., a Marie Curie IIF Fellowship to J.G., and the  
269 Max Planck Society to J.G. The funders had no role in study design, data collection and  
270 interpretation, or the decision to submit the work for publication. Any opinions, findings,  
271 and conclusions or recommendations expressed in this paper are those of the authors and  
272 do not necessarily reflect the views of the funders.

273

#### 274 **ACKNOWLEDGEMENTS**

275 We thank Neerja Hajela for assistance in the lab; Justin Meyer for advice on experimental  
276 methods, sharing samples from the coevolution experiments, and valuable discussions;

277 and Rohan Maddamsetti, Caroline Turner, and Mike Wiser for comments on the  
278 manuscript.

279

## 280 **AUTHOR CONTRIBUTIONS**

281 A.R.B., R.M.S., and R.E.L. conceived the study. A.R.B., R.M.S., and J.G. performed the  
282 experiments. All authors analyzed the data and wrote the manuscript.

283

## 284 **CONFLICTS OF INTEREST**

285 The authors declare that there are no conflicts of interest.

286

## 287 **REFERENCES**

- 288 1. **Lenski RE, Levin BR.** 1985. Constraints on the coevolution of bacteria and virulent  
289 phage: a model, some experiments, and predictions for natural communities. *The*  
290 *American Naturalist* **125**:585-602.
- 291 2. **Chao L, Levin BR, Stewart FM.** 1977. A complex community in a simple habitat: an  
292 experimental study with bacteria and phage. *Ecology* **58**:369-378.
- 293 3. **Levin BR, Stewart FM, Chao L.** 1977. Resource-limited growth, competition, and  
294 predation: a model and experimental studies with bacteria and bacteriophage. *The*  
295 *American Naturalist* **111**:3-24.
- 296 4. **Waterbury JB, Valois FW.** 1993. Resistance to co-occurring phages enables marine  
297 *Synechococcus* communities to coexist with cyanophages abundant in seawater. *Applied*  
298 *and environmental microbiology* **59**:3393-3399.
- 299 5. **Smith HW, Huggins MB.** 1980. The association of the O18, K1 and H7 antigens and the  
300 CoIV plasmid of a strain of *Escherichia coli* with its virulence and immunogenicity.  
301 *Microbiology* **121**:387-400.
- 302 6. **Smith HW, Huggins MB.** 1982. Successful treatment of experimental *Escherichia coli*  
303 infections in mice using phage: its general superiority over antibiotics. *Journal of General*  
304 *Microbiology* **128**:307-318.
- 305 7. **Burmeister AR, Fortier A, Roush C, Lessing AJ, Bender RG, Barahman R, Grant**  
306 **R, Chan BK, Turner PE.** 2020. Pleiotropy complicates a trade-off between phage  
307 resistance and antibiotic resistance. *Proc Natl Acad Sci U S A* **117**:11207-11216.

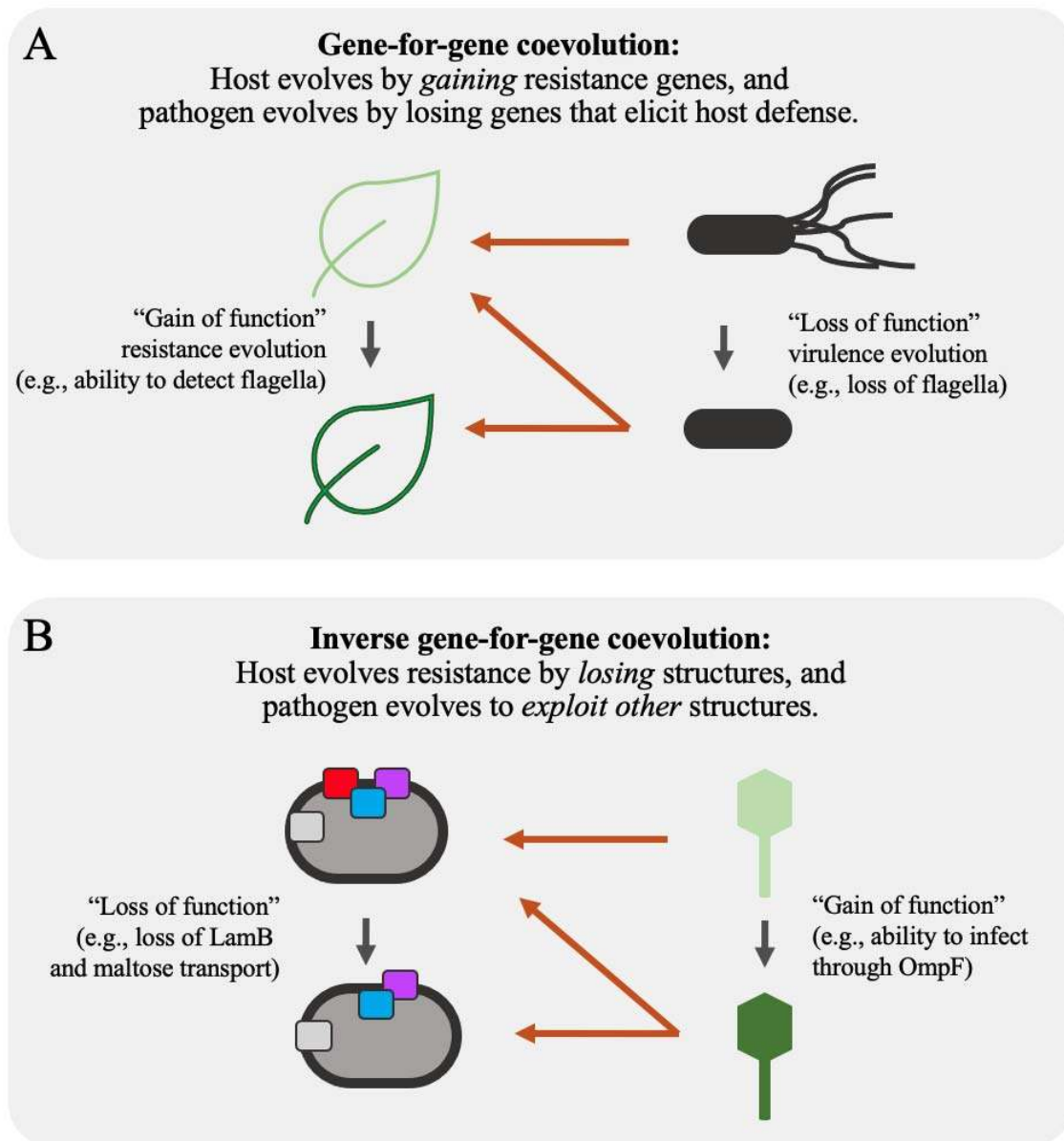
- 308 8. **Chan BK, Siström M, Wertz JE, Kortright KE, Narayan D, Turner PE.** 2016. Phage  
309 selection restores antibiotic sensitivity in MDR *Pseudomonas aeruginosa*. *Sci Rep*  
310 **6**:26717.
- 311 9. **Kortright KE, Chan BK, Koff JL, Turner PE.** 2019. Phage therapy: A renewed  
312 approach to combat antibiotic-resistant bacteria. *Cell Host Microbe* **25**:219-232.
- 313 10. **Barrangou R, Fremaux C, Deveau H, Richards M, Boyaval P, Moineau S, Romero**  
314 **DA, Horvath P.** 2007. CRISPR provides acquired resistance against viruses in  
315 prokaryotes. *Science* **315**:1709.
- 316 11. **Shmakov S, Smargon A, Scott D, Cox D, Pyzocha N, Yan W, Abudayyeh OO,**  
317 **Gootenberg JS, Makarova KS, Wolf YI, Severinov K, Zhang F, Koonin EV.** 2017.  
318 Diversity and evolution of class 2 CRISPR–Cas systems. *Nature Reviews Microbiology*  
319 **15**:169-182.
- 320 12. **Westra ER, Levin BR.** 2020. It is unclear how important CRISPR–Cas systems are for  
321 protecting natural populations of bacteria against infections by mobile genetic elements.  
322 *Proceedings of the National Academy of Sciences* **117**:27777-27785.
- 323 13. **Pawluk A, Davidson AR, Maxwell KL.** 2018. Anti-CRISPR: discovery, mechanism and  
324 function. *Nature Reviews Microbiology* **16**:12+.
- 325 14. **Buckling A, Rainey PB.** 2002. Antagonistic coevolution between a bacterium and a  
326 bacteriophage. *Proceedings of the Royal Society of London Series B: Biological Sciences*  
327 **269**:931-936.
- 328 15. **Scanlan PD, Buckling A.** 2012. Co-evolution with lytic phage selects for the mucoid  
329 phenotype of *Pseudomonas fluorescens* SBW25. *The ISME journal* **6**:1148-1158.
- 330 16. **Scanlan PD, Hall AR, Lopez-Pascua LDC, Buckling A.** 2011. Genetic basis of  
331 infectivity evolution in a bacteriophage. *Molecular Ecology* **20**:981-989.
- 332 17. **Meyer JR, Dobias DT, Weitz JS, Barrick JE, Quick RT, Lenski RE.** 2012.  
333 Repeatability and contingency in the evolution of a key innovation in phage lambda.  
334 *Science* **335**:428-432.
- 335 18. **Fenton A, Antonovics J, Brockhurst MA.** 2009. Inverse-gene-for-gene infection  
336 genetics and coevolutionary dynamics. *Am Nat* **174**:E230-242.
- 337 19. **Fenton A, Antonovics J, Brockhurst MA.** 2012. Two-step infection processes can lead  
338 to coevolution between functionally independent infection and resistance pathways.  
339 *Evolution* **66**:2030-2041.
- 340 20. **Sieber M, Robb M, Forde SE, Gudelj I.** 2014. Dispersal network structure and  
341 infection mechanism shape diversity in a coevolutionary bacteria-phage system. *ISME*  
342 *Journal* **8**:504-514.
- 343 21. **Agrawal A, Lively CM.** 2002. Infection genetics: gene-for-gene versus matching-alleles  
344 models and all points in between. *Evolutionary Ecology Research* **4**:79-90.

- 345 22. **Dennehy JJ.** 2012. What can phages tell us about host-pathogen coevolution? *Int J Evol*  
346 *Biol* **2012**:396165.
- 347 23. **Koskella B, Brockhurst MA.** 2014. Bacteria-phage coevolution as a driver of ecological  
348 and evolutionary processes in microbial communities. *FEMS Microbiol Rev* **38**:916-931.
- 349 24. **Chaudhry WN, Pleška M, Shah NN, Weiss H, McCall IC, Meyer JR, Gupta A, Guet**  
350 **CC, Levin BR.** 2018. Leaky resistance and the conditions for the existence of lytic  
351 bacteriophage. *PLOS Biology* **16**:e2005971.
- 352 25. **Hofnung M, Jezierska A, Braun-Breton C.** 1976. *lamB* mutations in *E. coli* K12:  
353 growth of lambda host range mutants and effect of nonsense suppressors. *Mol Gen Genet*  
354 **145**:207-213.
- 355 26. **Thirion JP, Hofnung M.** 1972. On some genetic aspects of phage lambda resistance in  
356 *E. coli* K12. *Genetics* **71**:207-216.
- 357 27. **Elliott J, Arber W.** 1978. *E. coli* K-12 *pel* mutants, which block phage lambda DNA  
358 injection, coincide with *ptsM*, which determines a component of a sugar transport system.  
359 *Mol Gen Genet* **161**:1-8.
- 360 28. **Erni B, Zanolari B, Kocher HP.** 1987. The mannose permease of *Escherichia coli*  
361 consists of three different proteins: amino acid sequence and function in sugar transport,  
362 sugar phosphorylation, and penetration of phage lambda DNA. *J Biol Chem* **262**:5238-  
363 5247.
- 364 29. **Esquinas-Rychen M, Erni B.** 2001. Facilitation of bacteriophage lambda DNA injection  
365 by inner membrane proteins of the bacterial phosphoenol-pyruvate: carbohydrate  
366 phosphotransferase system (PTS). *J Mol Microbiol Biotechnol* **3**:361-370.
- 367 30. **Scandella D, Arber W.** 1974. An *Escherichia coli* mutant which inhibits the injection of  
368 phage lambda DNA. *Virology* **58**:504-513.
- 369 31. **Spanakis E, Horne MT.** 1987. Co-adaptation of *Escherichia coli* and coliphage  $\lambda$ vir in  
370 continuous culture. *J Gen Microbiol* **133**:353-360.
- 371 32. **Meyer JR, Agrawal AA, Quick RT, Dobias DT, Schneider D, Lenski RE.** 2010.  
372 Parallel changes in host resistance to viral infection during 45,000 generations of relaxed  
373 selection. *Evolution* **64**:3024-3034.
- 374 33. **Burmeister AR, Lenski RE, Meyer JR.** 2016. Host coevolution alters the adaptive  
375 landscape of a virus. *Proc Roy Soc B: Biol Sci* **283**:20161528.
- 376 34. **Meyer JR, Flores CO, Weitz JS, Lenski RE.** 2008. Key innovation in a virus catalyzes  
377 a coevolutionary arms race. *ALife Proceedings* **13**:532-533.
- 378 35. **Baba T, Ara T, Hasegawa M, Takai Y, Okumura Y, Baba M, Datsenko KA, Tomita**  
379 **M, Wanner BL, Mori H.** 2006. Construction of *Escherichia coli* K-12 in-frame, single-  
380 gene knockout mutants: the Keio collection. *Mol Syst Biol* **2**:2006 0008.



- 381 36. **Burmeister AR, Sullivan R, Lenski RE.** 2020. Fitness costs and benefits of resistance  
382 to phage lambda in experimentally evolved *Escherichia coli*, p 123-143. In Banzhaf W,  
383 Cheng B, Deb K, Holekamp K, Lenski RE, Ofria C, Pennock R, Punch B, Whittaker D  
384 (ed), *Evolution in action: past, present, and future*. Springer, New York, NY.
- 385 37. **Williams N, Fox DK, Shea C, Roseman S.** 1986. Pel, the protein that permits lambda  
386 DNA penetration of *Escherichia coli*, is encoded by a gene in *ptsM* and is required for  
387 mannose utilization by the phosphotransferase system. *Proc Natl Acad Sci U S A*  
388 **83**:8934-8938.
- 389 38. **Scandella D, Arber W.** 1976. Phage lambda-DNA injection into *Escherichia coli pel*-  
390 mutants is restored by mutations in phage gene *V* or gene *H*. *Virology* **69**:206-215.
- 391 39. **Gupta A, Peng S, Leung CY, Borin JM, Weitz JS, Meyer JR.** 2020. Leapfrog  
392 dynamics in phage-bacteria coevolution revealed by joint analysis of cross-infection  
393 phenotypes and whole genome sequencing. bioRxiv  
394 doi:10.1101/2020.10.31.337758:2020.2010.2031.337758.  
395
- 396

397 **Figures**



398

399 **Fig. 1.** Genetic interaction networks during gene-for-gene (GFG) coevolution  
400 (panel A) and inverse-gene-for-gene (IGFG) coevolution (panel B). In both  
401 scenarios, host alleles affect selection on pathogen phenotypes, and pathogen  
402 alleles influence selection on host phenotypes. However, the two models have  
403 different implications for understanding historical coevolution and predicting

404 future changes. During GFG coevolution, hosts evolve resistance by gaining  
405 resistance genes, and pathogens evolve by losing genes that elicit host  
406 defenses. GFG coevolution is common among plants and their bacterial  
407 pathogens; it may also occur in bacteria-phage interactions that involve  
408 restriction-modification and CRISPR defenses. During IGFG coevolution,  
409 pathogen infectivity requires the exploitation of specific host features, and  
410 resistance involves eliminating the exploited features. Unlike in the GFG model,  
411 host defenses in the IGFG model do not require pathogen recognition, and the  
412 pathogen's evasion of host resistance does not require the loss of a defense  
413 elicitor.

414

415

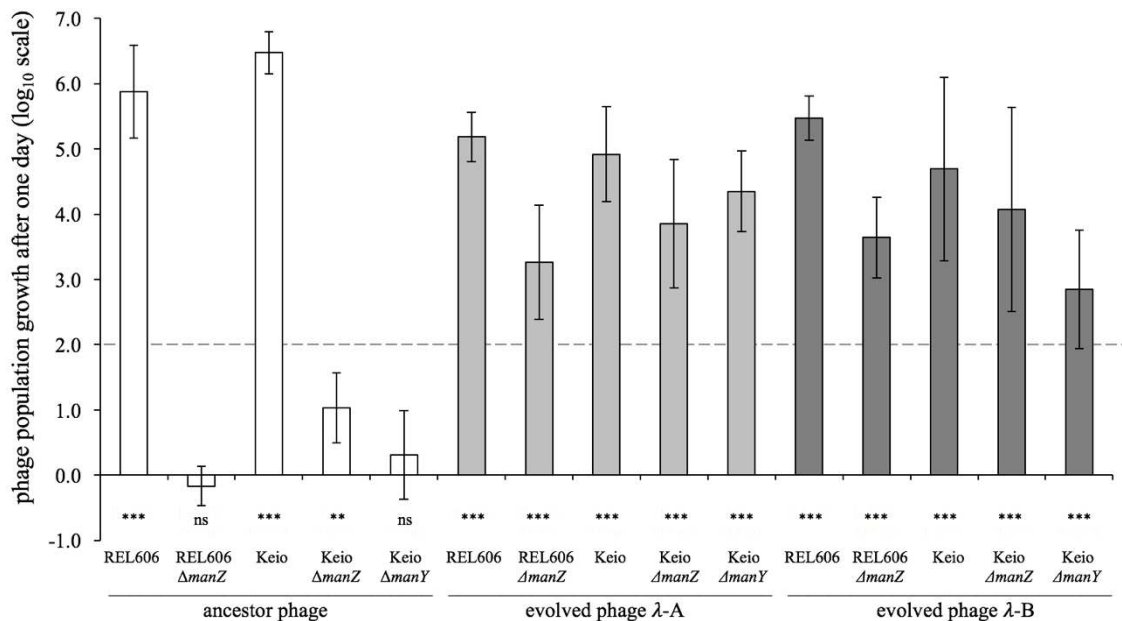
416

417

418

419

420



421

422 **Fig. 2.** Net population growth of phage  $\lambda$  on wild type,  $\Delta manY$ , and  $\Delta manZ$

423 bacteria. Whether the phage could grow was assessed by performing one-tailed

424 *t*-tests on the log<sub>10</sub>-transformed ratio of phage population densities at the start

425 and end of a one-day cycle, with the null hypothesis of zero growth (\*\*\*,  $p <$

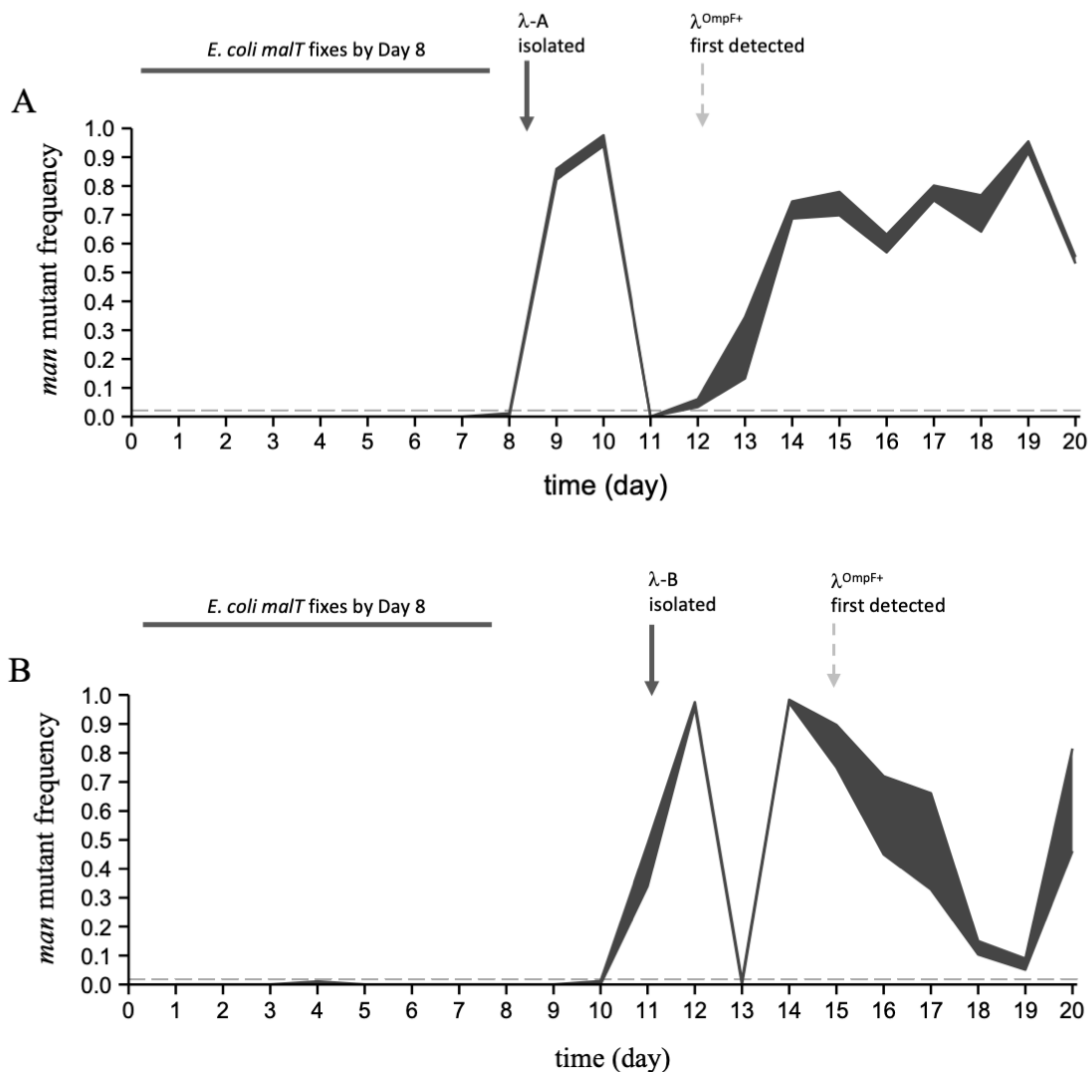
426 0.001; \*\*,  $0.001 < p < 0.01$ ; ns, not significant,  $p > 0.05$ ). Each test was based on

427 5 or 6 replicate assays. Phage isolates  $\lambda$ -A and  $\lambda$ -B evolved in a batch-culture

428 regime with 100-fold dilution each day, and so 100-fold growth was required for

429 their persistence; this break-even level is indicated by the dashed line.

430



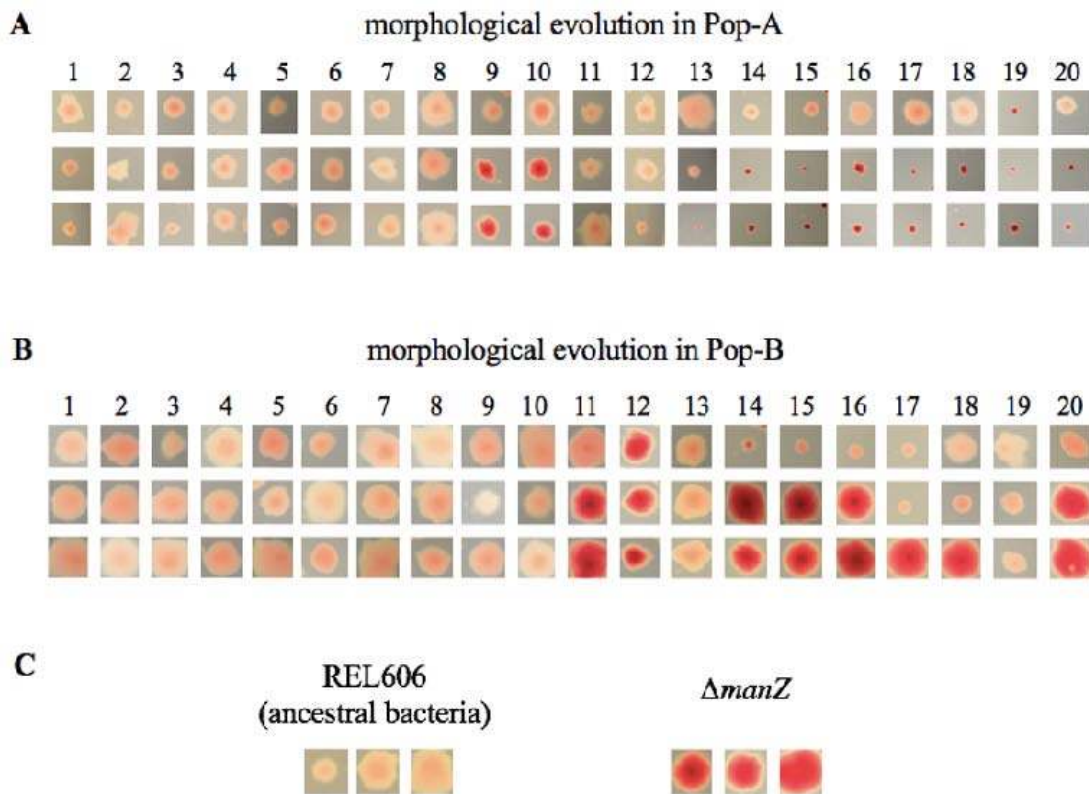
431

432 **Fig. 3.** Temporal dynamics of *man* mutants in *E. coli* populations Pop-A (panel A)  
433 and Pop-B (panel B). Mutant *malT* alleles had already reached fixation in both  
434 populations by day 8 (17). Bacteria with *man* mutations, which confer resistance  
435 to the ancestral phage  $\lambda$ , rose to high frequencies and then declined sharply in  
436 abundance in both populations after day 8, but before  $\lambda$  had evolved to use the  
437 alternative receptor OmpF (timing indicated by vertical dashed arrows). These  
438 data imply that the *man* mutations evolved on *malT* mutant backgrounds, and  
439 that  $\lambda$  evolved independence of the mannose permease – causing the

440 precipitous decline in the frequency of *man* mutants – before it evolved the ability  
441 to use OmpF. The shaded regions indicate the maximum and minimum  
442 frequencies of the *man* mutants based on analyzing two samples per population  
443 each day (mean  $N = 90$  colonies tested per sample, minimum 29 colonies). The  
444 horizontal gray dashed lines show the approximate limit of detection of the *man*  
445 mutants (0.019 for panel A, 0.022 for panel B).

446

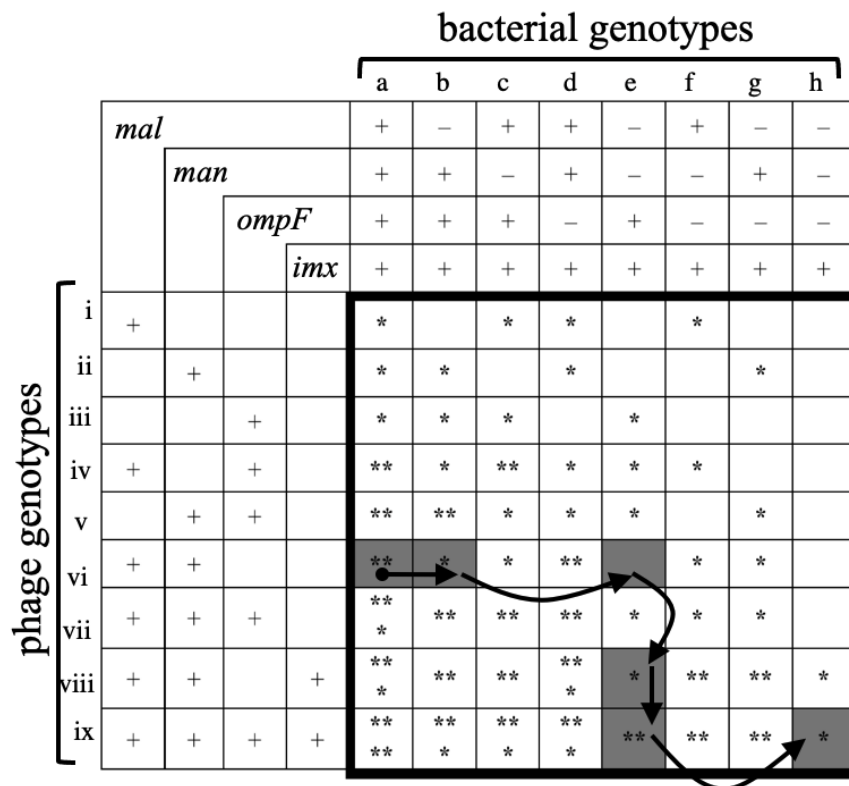
447



448

449 **Fig. 4.** Evolution of *man*-related colony morphology on tetrazolium mannose  
450 agar. *E. coli* mutants with reduced ability to metabolize mannose form more  
451 deeply pigmented colonies than the wild type bacteria. Three representative  
452 colonies are shown for each sample from days 1-20 of two coevolution  
453 experiments. Representative colonies within a column are from the same agar  
454 plate and shown at the same magnification after incubation for 18-21 hours.  
455 Panel A: Pop-A. Panel B: Pop-B. Panel C: Comparison of wild type and  $\Delta manZ$   
456 bacteria in the same *E. coli* strain B genetic background.

457



458

459 **Fig. 5.** An inverse-gene-for-gene model showing the structure of the genetic  
 460 network for coevolving *E. coli* and  $\lambda$  populations. Columns indicate bacterial  
 461 genotypes with four exploitable features, and rows indicate  $\lambda$  genotypes that  
 462 exploit those features: *mal*, maltose transport across the outer membrane; *man*,  
 463 mannose transport across the inner membrane; *ompF*, glucose and electrolyte  
 464 transport across the outer membrane; *imx*, a hypothetical inner membrane  
 465 feature that is exploited by  $\lambda$  that evolved independence of the mannose  
 466 permease. The "+" symbol indicates that either the bacteria have the feature or  
 467 the phage exploit the feature. The "-" symbol indicates the bacteria lack the  
 468 feature, express it to a reduced degree, or otherwise modify it to minimize phage  
 469 infection. Asterisks (\*) indicate infectivity for each host-phage pair, with more  
 470 asterisks indicating greater infectivity. Adaptive changes through the network can



471 proceed by two types of moves: *E. coli* resistance (to the right across rows), and  
472 increased  $\lambda$  infectivity (downward across columns). The coevolving communities  
473 were founded by host genotype a and phage genotype vi (shown by the black  
474 circle). The communities analyzed in this study appear to have moved through  
475 the shaded nodes in five steps, as indicated by the arrows.

476

477 **Tables**

478 **Table 1.** *E. coli* and phage  $\lambda$  strains used in this study.

Strain	Description	Relevant Characteristics
<b>Bacteria Clones:</b>		
REL606	<i>E. coli</i> B ancestor of coevolution experiment	<i>malT</i> <sup>+</sup> , <i>ompF</i> <sup>+</sup> , <i>manY</i> <sup>+</sup> , <i>manZ</i> <sup>+</sup>
REL606 $\Delta$ <i>manZ</i>	<i>manZ</i> deletion, derived from REL606 <sup>a</sup>	$\Delta$ <i>manZ</i>
BW25113	<i>E. coli</i> K12 parental strain of Keio collection	<i>malT</i> <sup>+</sup> , <i>ompF</i> <sup>+</sup> , <i>manY</i> <sup>+</sup> , <i>manZ</i> <sup>+</sup>
JW1807	<i>manY</i> deletion in Keio collection	$\Delta$ <i>manY</i>
JW1808	<i>manZ</i> deletion in Keio collection	$\Delta$ <i>manZ</i>
DH5 $\alpha$	Strain used for $\lambda$ plaque-based enumeration	<i>malT</i> <sup>+</sup> , <i>ompF</i> <sup>+</sup> , <i>manY</i> <sup>+</sup> , <i>manZ</i> <sup>+</sup>
<b>Phage Clones:</b>		
cI26	Lytic $\lambda$ ancestor of both phage populations	Requires <i>E. coli</i> LamB
$\lambda$ -A	Evolved $\lambda$ isolate from Pop-A <sup>b</sup> on Day 8 (4 days before the population evolved to use OmpF)	Requires <i>E. coli</i> LamB
$\lambda$ -B	Evolved $\lambda$ isolate from Pop-B <sup>b</sup> on Day 11 (4 days before the population evolved to use OmpF)	Requires <i>E. coli</i> LamB

479 <sup>a</sup>This strain also has three mutations that have no known relevance to interactions with phage  $\lambda$   
480 (Supplementary Material). For construction methods, see Supplementary Material, Table S1, and Table S2.

481 <sup>b</sup>For simplicity, we have designated the source populations Pop-A and Pop-B. These correspond to  
482 population numbers D9 and G9 in the original experiment described by Meyer *et al.* (17).

483

484